Lattice distortion induced site dependent carbon gettering at twin boundaries in silicon

Dongdong Zhao[a], Yanjun Li[*,a]

[a]*Department of Materials Science and Engineering, Norwegian University of Science and Technology (NTNU), 7491 Trondheim, Norway*

*Corresponding author. E-mail: yanjun.li@ntnu.no Tel.: +47 73551206

Abstract

The interactions between substitutional carbon atoms and Σ3 {111}, Σ9 {221}, and Σ27 {552} twin boundaries (TB) in silicon were investigated by first-principles calculations. The preferential segregation sites and segregation energy for carbon at different TBs were determined. It shows that segregation of carbon atoms at Σ3 {111} TB is energetically unfavorable while Σ9 {221} and Σ27 {552} TBs are efficient gettering centers for carbon. A linear relationship between the atomic-site specific segregation energy for carbon at TBs and the average bond length (ABL) of the atomic site is deduced.

Keywords: Carbon gettering, twin boundaries, segregation, mc-Si, first-principles calculations.

1. Introduction

Due to the low production cost, multi-crystalline Si (mc-Si) now accounts for over 50% of the feedstock materials for photovoltaic solar cells [1, 2]. However, solar cells based on casting mc-Si has a relatively high concentration of alien impurities [3-6], including transition metals (e.g. Fe, Cu, Cr, Ni, etc.) and light elements (e.g. C, O, N, etc.), most of which have detrimental effect on the solar cell efficiency [4, 5, 7-9]. C, usually inherited from crucible and furnace during casting process, is an inevitable impurity in mc-Si. Many experimental evidences demonstrate that C tends to segregate at structural defects and especially at grain boundaries (GBs) in mc-Si. For instance, Stoffers et al. [4] detected the remarkable C segregation at the Σ9 and Σ27 GBs, by using 3D atom probe tomography (APT) measurement and electron-beam-induced current (EBIC). The presence of C in mc-Si can significantly influence the electrical activity of GBs and dislocations, and thus affect the minority carrier properties of mc-Si [10, 11]. Also, the segregated C solutes at GBs can serve as gettering sites for harmful transitional impurities like Fe and Cu [12, 13], which is believed to benefit the solar cell performance in terms of internal gettering. Furthermore, the existence of C solutes can drastically enhance the precipitation of O during thermal annealing [14]. These precipitates can deteriorate solar cell efficiency and also serve as gettering centers for detrimental metallic contaminants [6]. Therefore, an in-depth fundamental understanding of the segregation behavior of C along GBs in mc-Si is of great importance to increase the efficiency of mc-Si based solar cells.

The impurity segregation at GBs is mainly controlled by the interaction energy between individual impurity and GBs. However, the interaction between impurities and GBs in mc-Si is rather complex and therefore difficult to investigate relying solely on experimental techniques like APT and EBIC [3, 5]. Fortunately, the rapid development of atomistic simulation approaches over the past decades has made it possible to achieve quantitative understanding on the individual impurity-GB interactions, in terms of specific atomic sites and the corresponding segregation energy [15, 16]. Nevertheless, such simulation work has been few, which is attributed to the key challenges with constructing the accurate GB structures in Si [17], as well as the high computational demands when it comes to high order coincidence site lattice (CSL) GBs [3] (e.g. Σ27 GBs in Si). The C-GB

interactions were once investigated by Käshammer and Sinno [3] using empirical molecular dynamics (EMD), they found these interactions were strongly correlated with the local atomic GB bonding network. However, considering the intrinsic uncertainty of empirical potentials, more reliable investigation approaches like density functional theory (DFT) calculations are needed to calculate the C-GB interactions in Si. A successful attempt by using first-principles calculations is the study of interstitial Fe segregation towards GBs in Si by Ziebarth et al. [8], in which the segregation of interstitial Fe impurity is revealed to be site specific at some special GBs, e.g. Σ3 {112} GBs.

The Σ3, Σ9, and Σ27 twin boundaries (TBs) are the mostly observed GBs in as-cast mc-Si, accounting for over 50% of the total GB population [18]. The first-order TB, Σ3 {111} is usually dislocation and stress free. The second order Σ9 {221} and third order Σ27 {552} TBs can form via sequential twinning reactions between the first order TBs [19]. In this work, the Σ3 {111}, Σ9 {221} and Σ27 {552} TBs were selected as the representative GBs to interpret the C-GB interactions in Si. DFT calculations were carried out to quantitatively reveal the underlining driving force for C gettering at GBs in mc-Si.

2. Computational details

All the DFT calculations in the present work were performed with Vienna ab initio simulation package (VASP) [20]. The exchange correlation functions were described with generalized gradient approximation (GGA) [21] in the Perdew–Burke–Ernzerhof form [22]. An energy cutoff of 400 eV was adopted in all the calculations to insure the total energy differences were less than 1 meV/atom. Monk-horst Pack *k*-points sampling was used for the Brillouin-zone integrals. Structural relaxations were performed until the Hellmann-Feynman force on all atoms was $< 10^{-2}$ eV·Å^{-1}. The linear tetrahedron method including Blöchl corrections [23] was utilized for the total energy calculations. In order to perform the calculations, 3D bicrystal type supercells containing 96, 136 and 216 atoms for Σ3 {111}, Σ9 {221} and Σ27 {552} TBs respectively were created according to the various experimental observations [24-26] and computational predictions [27]. In each bicrystal supercell, there are two TBs and two micro-grains separated by the TBs. The convergence of TB energy with

respect to increased supercell size and thus increased TB-TB spacing was evaluated in order to choose the adequate supercell size. Proper supercell size was selected on condition that the TB energy difference was converged to less than 5 mJ/m^2, wherein the artificial TB-TB interactions can be considered as being negligible. Convergence test also indicates that the *k*-points sampling dimension (cf. Table. 1) are adequate to yield well-converged results.

The interfacial energy γ_{TB} of the TBs were evaluated using

$$\gamma_{TB} = \left(E_{SiTB}^{tot} - N_{Si}\mu_{Si} \right) / 2A \tag{1}$$

In Eq. (1), E_{SiTB}^{tot} is the total free energy of a bicrystal cell and N_{Si} correspondingly, the number of Si atoms. μ_{Si} is the chemical potential per Si atom, calculated from the *diamond* phase. *A* is the cross-section area of the TB. The scaling factor ½ in Eq. (1) indicates the presence of two TBs in the bicrystal.

To quantify the interactions between C solutes and TBs, the segregation energy of C impurities at the TBs, γ_{seg}, was introduced and calculated based on

$$\gamma_{seg} = E_{ie}^{TB} - E_{ie}^{Bulk} \tag{2}$$

Where E_{ie}^{TB} is the impurity energy of carbon in a TB, and E_{ie}^{Bulk} correspondingly in bulk, the two of which can be calculated as

$$E_{ie}^{TB} = E_{TB}^{Si_{n-1}C_1} - E_{TB}^{Si_{n-1}} - \mu_C \tag{3}$$

$$E_{ie}^{Bulk} = E_{Bulk}^{Si_{n-1}C_1} - E_{Bulk}^{Si_{n-1}} - \mu_C \tag{4}$$

$E_{TB}^{Si_{n-1}C_1}$ is the total energy of a TB containing one C atom, $E_{TB}^{Si_{n-1}}$ stands for the total energy of pristine TB without C impurities, $E_{Bulk}^{Si_{n-1}C_1}$, $E_{Bulk}^{Si_{n-1}}$ for pure Si bulk with and without C impurity, respectively. μ_C is the chemical potential per C atom, evaluated from the *graphite* phase. A negative value of γ_{seg}

implies that it's energetically favorable for C impurity to segregate from bulk environment to TBs. It is worth noting that no energetically favorable sites has been identified for interstitial segregation of C atoms, thus we will mainly focus on the substitutional C segregation behavior along Si TBs.

3. Results and discussions

The relaxed interfacial structures of Σ3 {111}, Σ9 {221}, and Σ27 {552} TBs, shown in Fig. 1, are in good agreement with the experimental observations [24, 25, 28] and theoretical predictions [3, 8, 27]. Table 1 presents the calculated γ_{TB} of Σ3 {111}, Σ9 {221}, and Σ27 {552}. As can be seen, the γ_{TB} values of Σ3 {111} and Σ9 {221} obtained in this work are very close to the data by Ziebarth et al. [8] based on DFT calculations. In contrast, the γ_{TB} values of Σ9 {221}, and Σ27 {552} predicted by Käshammer and Sinno [3] using empirical potentials are much larger, which indicates that empirical descriptions of interatomic interactions tend to introduce uncertainties and leads to a larger predicted interfacial energies than DFT [29].

Interestingly, Σ3 {111} TB has an extremely low γ_{TB}, i.e. 0.014 J/m^2, which is attributed to the fact that the bonding structure of atoms (angle and length of bonds) at the TB is nearly the same as that in perfect bulk Si crystal. However the γ_{TB} values of Σ27 {552} and Σ9 {221} TBs are much higher than Σ3 {111} TB. This is due to the different atomic constructions in the higher order TBs. As indicated in Fig. 1(b) and (c), different from the 6-membered rings in Σ3 {111} TB, Σ9 {221} and Σ27 {552} TBs consist of 5- and 7-membered ring units, which introduces larger distortions of atomic bonding at TBs. The increase in γ_{TB} values of the TBs with increasing of twin order is consistent with the tendency predicted in Ref. [3].

The segregation energy profile of C solutes at distinct core sites along these TBs are displayed in Fig. 2. As can be seen from Fig. 1(a), due to the periodicity nature, there are only two distinct substitutional core sites in Σ3 {111} TB. A replacement of any of the two sites with C atoms will produce a positive γ_{seg} (cf. Fig. 2), which implies the C segregation at this TB is energetically unfavorable. This pronounced positive γ_{seg} should be attributed to the different lattice distortion behavior of Si bulk lattice and Σ3 {111} TB induced by C substitution. When one C atom is inserted

into Si bulk lattice, four Si-Si bonds are replaced by C-Si bonds, with a uniform bond length of 2.019 Å, however, the typical bulk bonding angle of 109.47° does not change. In contrast, C substitution at the core sites of Σ3 {111} TB not only alters the length of surrounding bonds, but also induces a pronounced change in the bonding angle of the site, in comparison to pristine Σ3{111} TB. It is worth noting that such a repulsive C-TB interaction is not surprising since the Σ3 {111} TB, having extremely low γ_{TB}, is quite stable and would reject any structural changes. The unfavorable C segregation at Σ3 {111} TB is consistent with the experimental results from APT analysis: no C segregation/enrichment was detected at the coherent Σ3 {111} TB [4], indicating that the Σ3 {111} TB does not possess any gettering ability of C solutes. Similar results have been found in the APT measurement by Ohno et al. [30], showing that Σ3 {111} TB is incapable to getter P, B, O and Cu atoms even when impurity concentration in the bulk is high. It has to be noted that the conclusion that Σ3 {111} TB is not a favorable segregation site for C is only valid for perfect straight Σ3 {111} TB. In mc-Si, the Σ3 {111} TB is sometimes distorted by extrinsic dislocations, resulting in deviation of the local twin boundary from the perfect Σ3 {111} TB misorientation [31]. These dislocations may serve as gettering centers for impurity atoms [32].

There are 8 distinct atomic core sites at Σ9 {221} TB and the interactions between C solutes and the TB is more complex. Among the 8 core sites, one site (site 5) was found to possess a negative γ_{seg} (cf. Fig. 2), i.e. -0.223 eV/atom, corresponding to an attractive interaction between C and Σ9 {221} TB. Due to the symmetric nature of the TB, site 5′ is equivalent to site 5 and has the same γ_{seg}. It means that Σ9 {221} TB has the gettering ability for carbon atoms. All the rest of the core atomic sites are carbon-repulsive. This is different from the molecular dynamics prediction results by Käshammer and Sinno [3], which showed that there are 3 or 6 attractive distinct core sites for C segregation depending upon the empirical potentials used. The predicted gettering ability of Σ9 {221} TB for C is consistent with the experimental work by Stoffers et al. [4]. Their APT analysis on three Σ9 {221} TBs showed a C enrichment at the TB.

The interactions between C solutes and Σ27 {552} TB is even more complicated. The Σ27 {552} TB has 20 distinct substitutional core sites for possible C segregation. As indicated in Fig. 1(c)

and Fig. 2, 8 core atomic sites exhibit negative γ_{seg}, 5 of which have γ_{seg} values similar to or even lower than that of the atomic site 5 at Σ9 {221} TB. This is in good agreement with the EBIC and APT measurement results by Stoffers et al. [4], which shows that the C gettering also occurs at Σ27 {552} TB. Site 12, as the joint of one 5-membered and two 6-membered rings, exhibits the maximum energy for attractive interaction with C, γ_{seg} of -0.524 eV/atom. With more distinct substitutional sites energetically favorable for C segregation and more negative γ_{seg}, Σ27 {552} TB is supposed to have a higher C gettering ability than Σ9 {221} TB.

Indeed, the calculations show that there is a correlation between the C segregation level and the TB character, i.e. the C segregation level is increasing with twin order, Σ3 {111} < Σ9 {221} < Σ27 {552}, which is in agreement with the general trend proposed by Stoffers et al. [4] and Buonassisi et al. [32]. To explore the reason for the big difference in γ_{seg} existing between distinct core sites at TBs, the atomic bonding structures of core site 9 and 12 at Σ27 {552} TB, corresponding to the most repulsive and most attractive interactions with C atoms are shown in Fig. 3(a) and (b) respectively. It is clearly shown that the main difference between the two sites is the length of atomic bonds connecting to the sites (the bonding angle are not so much distorted, 109.47 ± 6º), namely the extent of lattice distortion around the sites. The length of all the bonds connecting to site 9 is larger than site 12, implying that the lattice distortion extent may have a strong influence on γ_{seg} of each core site. To quantify the lattice distortion, average bond length (ABL), an average length of the four surrounding covalent bonds of each site, is introduced in this work. Fig. 3(c) displays the variation of γ_{seg} of C solutes and ABL at different atomic sites in Σ27 {552} TB. It is interesting to see that these two variables have nearly the same evolution tendency versus segregation sites. Fig. 3(d) shows the evolution of the calculated γ_{seg} of C solutes at all TBs as a function of ABL of the core sites along pristine TBs. Strikingly, an almost linear relationship exists between these two variables, where the segregation energy increases with ABL. A linear function between γ_{seg} and ABL (with unit: Å) can be deduced as

$$\gamma_{seg} = 18.1221 \cdot (\mathrm{ABL} - 2.3506) \quad (5)$$

where 2.3506 is very close to the experimental length of Si-Si covalent bonds, 2.3517 Å, in bulk Si (lattice constant a = 5.4309 Å). So this equation can be interpreted as if an atomic site in TB has an ABL less than the equilibrium Si-Si bond length in bulk Si crystal, it will have a negative γ_{seg} for C-gettering. Since the segregation energy was calculated as the energy difference between the state of one C atom replacing one Si atom at TB and the state with one C atom substituting one Si atom in bulk, Eq. (5) is also physically meaningful. Therefore Eq. (5) can be further written as

$$\gamma_{seg} = 18.1221 \cdot (\text{ABL} - 2.3517) \quad (6)$$

Though not shown, this linear relationship also well fits the data points in Fig. 3(d).

Such a correlation between the γ_{seg} and lattice distortion around an atomic site should be attributed to the bonding energy effect and the geometrical effect caused by the substitution with C atoms. Once a Si atom is replaced by a C atom at TB, the four Si-Si covalent bonds will be replaced by C-Si covalent bonds. As is known that the equilibrium length of C-Si covalent bonds in β-SiC (diamond cubic crystal structure) is 1.8878 Å, corresponding to the highest bonding energy [33]. However, in bulk Si crystal, it is impossible to form C-Si bonds with such a short length. Nevertheless, a segregation of C atoms to atomic sites with a short ABL along the TBs can results in a shorter length between Si and C atoms, referring to a higher bonding energy and therefore a more stable structure. So a segregation of C atoms to atomic sites at TB with a short ABL is energetically favorable.

Furthermore, as discussed in Ref. [3], lattice distortion can generate alternating localized tensile and compressive regions along the GB. The ABL dependence of γ_{seg} of C solutes should also be attributed to the strain fields caused by lattice distortion in the vicinity of TBs. Since C atom has a smaller radius than Si, it is energetically favorable for the substitutional C atoms to take up the core Si sites in TBs which possess a shorter ABL than 2.3517Å, namely the sites subjected to a compression stress field (e.g. site 12 in Σ27 {552} TB). This can release the localized residual stress, and thus lower the elastic strain energy of the TB. In contrast, if a C atom occupies the core sites with longer ABL, it will further increase the elastic strain energy in the local region of TBs. Therefore, the atomic

site specific γ_{seg} of C solutes at TBs is due to the intrinsic heterogeneous distribution of lattice distortion of the TBs, and the extent of lattice distortion of the TB can largely determine its gettering ability for C.

Apart from the frequently observed TBs in Si, small/large angle GBs, random GBs as well as high Σ value GBs also exist, along which C segregation were also observed [4]. Nevertheless, it remains an open question that whether the correlation between ABL and γ_{seg} of C solutes as depicted by Eq. (6) can be extended to describe the C gettering at these GBs on condition that the GB equilibrium structure is known. It is relatively safe to say that Eq. (6) is applicable to the C gettering at atomic sites in mc-Si, of which the bonding angle are not so much distorted in reference to the equilibrium counterpart, i.e. 109.47°, in bulk-Si. As a test of the validity of such a relationship, the γ_{seg} of C at two atomic sites adjacent to Σ27 {552} TB, labeled as 21 and 22 in Fig. 1(c) were evaluated. The ABL values for the two atomic sites are measured as 2.3378 and 2.3407 Å, respectively. By using Eq. (6), the γ_{seg} values for the two sites are calculated as -0.248 and -0.200 eV/atom, respectively. These values are very close to the values predicted by DFT calculation, i.e. -0.183 and -0.165 eV/atom, indicating the validity of Eq. (6) for C segregation. With the correlation shown by Eq. (6), it is possible that we can roughly evaluate the C gettering ability of other GBs with known atomic structure by calculating the ABL of different atomic sites without simulating the specific interactions between C solutes and GBs in Si, which may probably tend to make the evaluation of C gettering ability of different GBs or even dislocations easier. However, in spite of this knowledge of the C-TB interactions in mc-Si, further calculations focusing on the C gettering at small/large angle GBs, random GBs as well as high Σ value GBs on the atomic and electronic scale is needed to address the C-GB interactions in mc-Si with a clearer manner.

4. Conclusions

In summary, the atomic site dependent gettering of C at Σ3 {111}, Σ9 {221}, and Σ27 {552} TBs in silicon was systematically investigated using first-principles calculations. The calculation results show that the Σ3 {111} TB is not able to getter C impurity, while C gettering could occur at Σ9

{221} and Σ27 {552} TBs, whereas Σ27 {552} TB exhibits a higher gettering ability. The prediction results are consistent with experimental observations. Further analysis reveals that the local compressive lattice distortion at the TBs provides the driving force for C gettering at specific atomic sites. A universal linear correlation between γ_{seg} of C solutes and the ABL of atomic sites along pristine TBs is obtained, which might possibly also be applicable to predict the segregation/gettering behavior of C solutes along other GBs or at dislocations in Si. This work provides an important and fundamental understanding towards the C gettering behavior at Si TBs, which is highly important for the photovoltaic applications of mc-Si.

Acknowledgements

This work is financially supported under the FRINATEK project 'BENTMAT' (project number 222173) from the Research Council of Norway. Computation time from the NOTUR consortium is gratefully acknowledged.

References

[1] T. Buonassisi, A.A. Istratov, M.D. Pickett, M. Heuer, J.P. Kalejs, G. Hahn, M.A. Marcus, B. Lai, Z. Cai, S.M. Heald, T.F. Ciszek, R.F. Clark, D.W. Cunningham, A.M. Gabor, R. Jonczyk, S. Narayanan, E. Sauar, E.R. Weber, Chemical Natures and Distributions of Metal Impurities in Multicrystalline Silicon Materials, Prog. Photovolt: Res. Appl., 14 (2006) 513–531.

[2] S. Joonwichien, I. Takahashi, K. Kutsukake, N. Usami, Effect of grain boundary character of multicrystalline Si on external and internal (phosphorus) gettering of impurities, Prog. Photovolt: Res. Appl., 24 (2016) 1615–1625.

[3] P. Käshammer, T. Sinno, Interactions of twin boundaries with intrinsic point defects and carbon in silicon, J. Appl. Phys., 114 (2013) 083505.

[4] A. Stoffers, O. Cojocaru-Mirédin, W. Seifert, S. Zaefferer, S. Riepe, D. Raabe, Grain boundary segregation in multicrystalline silicon: correlative characterization by EBSD, EBIC, and atom probe tomography, Prog. Photovolt: Res. Appl., 23 (2015) 1742–1753.

[5] P. Käshammer, T. Sinno, A mechanistic study of impurity segregation at silicon grain boundaries, J. Appl. Phys., 118 (2015) 095301.

[6] Y. Ohno, K. Inoue, K. Fujiwara, M. Deura, K. Kutsukake, I. Yonenaga, Y. Shimizu, K. Inoue, N. Ebisawa, Y. Nagai, Three-dimensional evaluation of gettering ability for oxygen atoms at small-angle tilt boundaries in Czochralski-grown silicon crystals, Appl. Phys. Lett., 106 (2015) 251603.
[7] A. Autruffe, L. Arnberg, M.D. Sabatino, Coincident site lattice bi-crystals growth—Impurity segregation towards grain boundaries, J. Cryst. Growth., (2015) 8-11.
[8] B. Ziebarth, M. Mrovec, C. Elsässer, P. Gumbsch, Interstitial iron impurities at grain boundaries in silicon: A first-principles study, Phys. Rev. B, 91 (2015) 035309.
[9] B. Chen, J. Chen, T. Sekiguchi, M. Saito, K. Kimoto, Structural characterization and iron detection at Σ3 grain boundaries in multicrystalline silicon, J. Appl. Phys., 105 (2009) 113502.
[10] S. Pizzini, A. Sandrinelli, M. Beghi, D. Narducci, F. Allegretti, S. Torchio, G. Fabbri, G.P. Ottaviani, F. Demartin, A. Fusi, Influence of Extended Defects and Native Impurities on the Electrical Properties of Directionally Solidified Polycrystalline Silicon, J. Electrochem. Soc., 135 (1988) 155-165.
[11] S. Pizzini, P. Cagnoni, A. Sandrinelli, M. Anderle, R. Canteri, Grain boundary segregation of oxygen and carbon in polycrystalline silicon, Appl. Phys. Lett., 51 (1987) 676-678.
[12] H. Wong, N.W. Cheung, P.K. Chu, Gettering of gold and copper with implanted carbon in silicon, Appl. Phys. Lett., 52 (1988) 889-891.
[13] W. Skorupa, R.A. Yankov, Carbon-mediated effects in silicon and in silicon-related materials, Mater. Chem. Phys., 44 (1996) 101-144.
[14] H.J. Möller, L. Long, M. Werner, D. Yang, Oxygen and Carbon Precipitation in Multicrystalline Solar Silicon, phys. stat. sol. (a), 171 (1999) 175-189.
[15] J. Zhang, Y.C. Dou, Y. Zheng, Twin-boundary segregation energies and solute-diffusion activation enthalpies in Mg-based binary systems: A first-principles study, Scr. Mater., 80 (2014) 17–20.
[16] N.C. Eurich, P.D. Bristowe, Segregation of alloying elements to intrinsic and extrinsic stacking faults in r'-Ni3Al via first principles calculations, Scr. Mater., 102 (2015) 87–90.
[17] H.-J. Möller, <011> tilt boundaries in the diamond cubic lattice, Phil. Mag. A, 43 (1981) 1045-1055.
[18] G. Stokkan, Twinning in multicrystalline silicon for solar cells, J. Crys. Growth., 384 (2013) 107–113.
[19] A. Garg, W.A.T. Clark, J.P. Hirth, Dissociated and faceted large-angle coincident-site-lattice boundaries in silicon, Phil. Mag. A, 59 (1989) 479-499.
[20] G. Kresse, J. Furthmüller, Efficient iterative schemes for ab initio total-energy calculations using a plane-wave basis set, Phys. Rev. B, 54 (1996) 11169-11186.
[21] P.E. Blöchl, Projector augmented-wave method, Phys. Rev. B, 50 (1994) 17953-17979.
[22] J.P. Perdew, K. Burke, M. Ernzerhof, Generalized Gradient Approximation Made Simple, Phys. Rev. Lett., 77 (1996) 3865.

[23] P.E. Blöchl, O. Jepsen, O.K. Andersen, Improved tetrahedron method for Brillouin-zone integrations, Phys. Rev. B, 49 (1994) 16223-16233
[24] B. Cunningham, H.P. Strunk, D.G. Ast, High resolution electron microscopy of a R=27 boundary in Silicon, Scr. Metall., 16 (1982) 349-352.
[25] M.D. Vaudin, B. Cunningham, D.G. Ast, The structure of second and third order twin boundaries in Silicon, Scr. Metall., 17 (1983) 191-198.
[26] H.J. Queisser, Properties of Twin Boundaries in Silicon, J. Electrochem. Soc., 110 (1963) 52-56.
[27] M. Kohyama, R. Yamamoto, M. Doyama, Structures and Energies of Symmetrical <011> Tilt Grain Boundaries in Silicon, Phys. Stat. Sol. (b), 137 (1986) 11-20.
[28] M. Couillard, G. Radtke, G.A. Botton, Strain fields around dislocation arrays in a Σ9 silicon bicrystal measured by scanning transmission electron microscopy, Phil. Mag. A, 93 (2013) 1250–1267.
[29] A. Stoffers, B. Ziebarth, J. Barthel, O. Cojocaru-Mirédin, C. Elsässer, D. Raabe, Complex Nanotwin Substructure of an Asymmetric Σ9 Tilt Grain Boundary in a Silicon Polycrystal, Phys. Rev. Lett., 115 (2015) 235502.
[30] Y. Ohno, K. Inoue, Y. Tokumoto, K. Kutsukake, I. Yonenaga, N. Ebisawa, H. Takamizawa, Y. Shimizu, K. Inoue, Y. Nagai, H. Yoshida, S. Takeda, Three-dimensional evaluation of gettering ability of Σ3 {111} grain boundaries in silicon by atom probe tomography combined with transmission electron microscopy, Appl. Phys. Lett., 103 (2013) 102102.
[31] H.Y. Wang, N. Usami, K. Fujiwara, K. Kutsukake, K. Nakajima, Microstructures of Si multicrystals and their impact on minority carrier diffusion length, Acta Mater., 57 (2009) 3268–3276.
[32] T. Buonassisi, A.A. Istratov, M.D. Pickett, M.A. Marcus, T.F. Ciszek, E.R. Weber, Metal precipitation at grain boundaries in silicon: Dependence on grain boundary character and dislocation decoration, Appl. Phys. Lett., 89 (2006) 042102.
[33] J. Dong, A.-B. Chen, Fundamental Properties of SiC: Crystal Structure, Bonding Energy, Band Structure, and Lattice Vibrations, 2004.

Tables

Table 1. Interfacial energy γ_{TB}, of Σ3 {111}, Σ9 {221}, and Σ27 {552} TBs. The previous theoretical data are also included for comparison.

Twin boundary	Misorientation angle, θ	Number of atoms	*k*-points sampling dimension	Twin boundary energy, γ_{TB}, J/m^2		
				This work (DFT)	[a]Ziebarth (DFT)	[b]Käshammer (EMD)
Σ3{111}	**70.53°**	**96**	**9×2×13**	**0.014**	**0.01**	**0.00**
Σ9{221}	**38.94°**	**136**	**7×2×15**	**0.183**	**0.16**	**[c]0.45, 0.52**
Σ27{552}	**31.59°**	**216**	**2×2×11**	**0.359**	**-**	**[c]0.58, 0.59, 0.66**

[a]from Ref. [8].

[b]from Ref. [3].

[c]γ_{TB} produced with different empirical potentials.

Figure captions

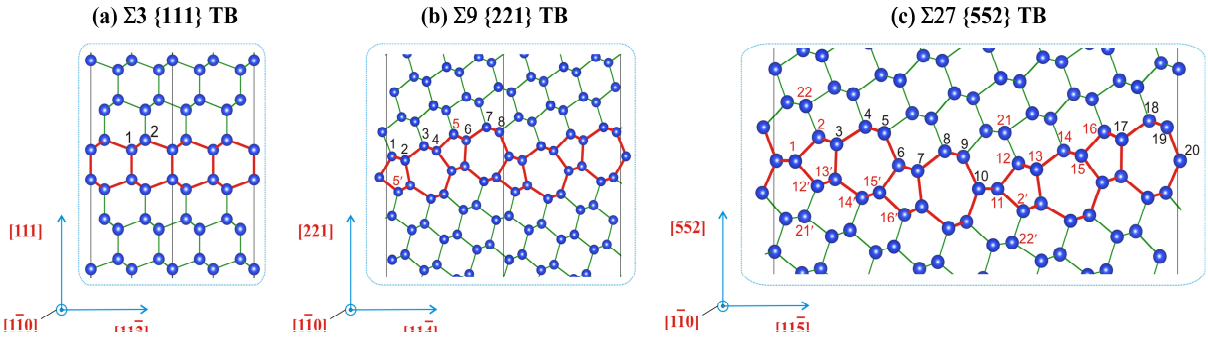

Fig. 1. Twin boundary core structures as projected in the $<1\bar{1}0>$ lattice direction, (a) Σ3 {111}, (b) Σ9 {221}, (c) Σ27 {552}. The core sites of each twin boundary are labelled with numbers for potential segregation of carbon. Structure units of the three twin boundaries are marked with red atomic bonds. Core sites with negative carbon segregation energy are labelled red.

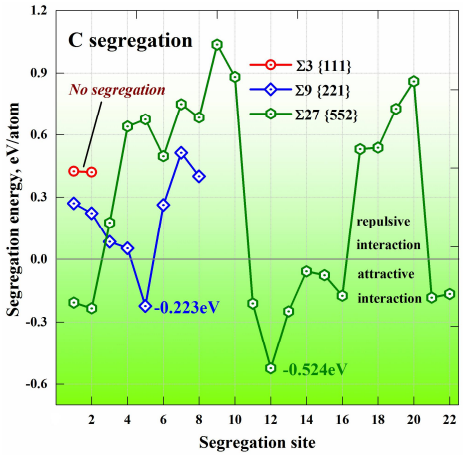

Fig. 2. Segregation energy of carbon at Σ3 {111}, Σ9 {221}, and Σ27 {552}. The energy is in eV/atom. The segregation sites of each twin boundary correspond to the core sites as indicated in Fig. 1.

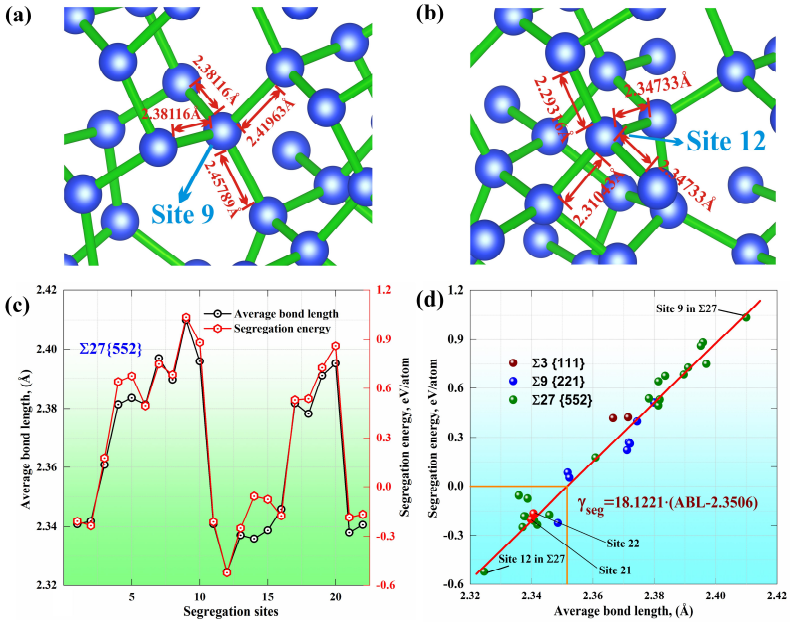

Fig. 3. (a) Bonding environment of site 9 in pristine Σ27 {552} TB. (b) Bonding environment of site 12 in pristine Σ27 {552} TB. (c) Average bond length versus segregation energy of carbon for different sites in Σ27 {552} TB. (d) Segregation energy of carbon at Σ3 {111}, Σ9 {221}, and Σ27 {552} TBs as a function of average bond length (ABL) for the segregation sites in the present work. The energy is in eV/atom.